AIAA JOURNAL
Vol. 44, No. 7, July 2006

Technical Notes

TECHNICAL NOTES are short manuscripts describing new developments or important results of a preliminary nature. These Notes should not exceed 2500 words (where a figure or table counts as 200 words). Following informal review by the Editors, they may be published within a few months of the date of receipt. Style requirements are the same as for regular contributions (see inside back cover).

Eddy Viscosity Transport Model Based on Elliptic Relaxation Approach

Branislav Basara*
AVL List, GmbH, 8020 Graz, Austria

DOI: 10.2514/1.20739

I. Introduction

THE modeling of near-wall turbulence with the k–ε model usually has two major problems: An inclusion of a distance to the wall as an explicit parameter and an improper boundary condition for the dissipation rate ε. The first problem makes the model inappropriate to simulate complex flows involving multiple surfaces. The second problem, as pointed out by Speziale et al. [1], has resulted in the use of a variety of derived boundary conditions that are asymptotically inconsistent or numerically stiff (e.g., zero normal derivatives of dissipation, links between dissipation, and derivatives of the turbulent kinetic energy, etc.). There are various proposals for the solution of both of these problems. On one hand, a number of low-Re number k–ε models have been proposed which use empirical functions to account for near-wall turbulence without using the explicit wall distance as a parameter. And on the other hand, a dissipation equation ε is replaced with $\omega(\omega \sim \varepsilon/k)$, $\tau(\tau = k/\varepsilon)$, and $\nu_t(\nu_t \sim k^2/\varepsilon)$ to simplify the employment of the wall boundary conditions. This has resulted in models known as k–ω (Wilcox [2]), k–τ (Speziale et al. [1]), ν_t–k (Peng and Davidson [3]), etc. However, an integration of governing equations up to the wall has never been accepted for practical engineering applications, bearing in mind that computational meshes usually do not satisfy a strict criteria for the position of the cells next to the wall. This criteria is necessary so that the low-Reynolds number models can successfully describe the viscous sublayer and the buffer region. And although computing power continues to increase allowing computational meshes to be finer than ever, standard industrial applications will be done using the wall function approach. The universal solution is to provide the wall approach which combines the integration up to the wall with wall functions. Recently the various proposals, e.g., the automatic wall treatment (Esch and Menter [4]), compound wall treatment (Popovac and Hanjalic [5]), etc., have provided an optimum solution for any computational mesh.

The $\overline{v^2}$–f of Durbin [6] has become increasingly popular as empirical damping functions are removed due to the employment of an additional velocity scale $\overline{v^2}$ derived by using an elliptic relaxation concept. However, the original model introduces the wall boundary condition for the elliptic relaxation function f proportional to $1/y^4$ (y is a wall distance) making computations more sensitive on very near-wall cells. Recently, two groups of authors, Hanjalic et al. [7] and Laurence et al. [8] made a similar, more robust formulation of the $\overline{v^2}$–f model. They proposed an eddy viscosity model which solves a transport equation for the velocity scale ratio $\overline{v^2}/k$ instead of $\overline{v^2}$. Therefore, the efficiency of the elliptic relaxation concept of Durbin [6] is kept which sensitizes $\overline{v^2}$ to the inviscid wall blocking effect, but the more robust wall boundary condition for the f equation is introduced, this time f_{wall} is proportional to $1/y^2$. Furthermore, the production of turbulence kinetic energy appears in the $\overline{v^2}/k$ equation while a dissipation rate ε is in the $\overline{v^2}$ equation which is much more difficult to reproduce accurately in the near-wall layer. Hanjalic et al. [7] made even further simplifications by modifying the model's constants to reduce the $\overline{v^2}/k$ equation to a source-sink diffusion form (see original reference). From the numerical aspects, solving $\overline{v^2}/k$ is also more robust as the maximum of this variable can be fixed on the physical limit equal to 2 [as $k = 0.5^*(\overline{u^2} + \overline{v^2} + \overline{w^2})$]. It is also clear and these authors stated that as well that the ζ–f or the $\overline{v^2}$–f models are still inferior to the Reynolds-stress model or even some nonlinear k–ε models and algebraic stress models for the calculations of particular flows and flow regions (e.g., three-dimensional flows with strong secondary motion, swirl or rotation, etc.), but much more accurate than the near-wall k–ε models or similar two-equation models. At the same time, these models are more robust than any Reynolds-stress models or even two-equations nonlinear k–ε models or algebraic stress models. Furthermore, these models represent an ideal choice when used in conjunction with the universal wall approach as for example proposed by Popovac and Hanjalic [5] related to their compound treatment of wall boundary conditions which combines the integration up to the wall with wall functions.

The work presented here further simplifies the approach of Popovac and Hanjalic [5]. This is done by introducing the eddy viscosity transport equation instead of the dissipation rate equation [see the work of Peng and Davidson [3] (PD) who derived a two-equation ν_t–k model]. Here, the elliptic relaxation approach is adopted for the k–$\tilde{\nu}_t$–ζ–f model and consequently, the compound wall treatment can be introduced very simply without modification for different variables.

II. Model Formulation

The Hanjalic et al. [7] ζ–f model was used as a starting point for the work presented here. In this model the eddy viscosity is defined as

$$\nu_t = C_\mu \zeta k \tau \tag{1}$$

The time scale τ is given as

$$\tau = \max\left[\min\left(\frac{k}{\varepsilon}, \frac{a}{\sqrt{6}C_\mu S\zeta}\right), C_\tau\left(\frac{\nu}{\varepsilon}\right)^{1/2}\right] \tag{2}$$

where $S = \sqrt{S_{ij}S_{ij}}$ and the mean-strain rate is

$$S_{ij} = \frac{1}{2}\left(\frac{\partial U_i}{\partial x_j} + \frac{\partial U_j}{\partial x_i}\right) \tag{3}$$

The coefficients appearing in Eqs. (1) and (2) take the values $a = 0.6$, $C_\mu = 0.22$, and $C_\tau = 6.0$. The complete model is given by the following equations:

$$\frac{Dk}{Dt} = P_k - \varepsilon + \frac{\partial}{\partial x_j}\left[\left(\nu + \frac{\nu_t}{\sigma_k}\right)\frac{\partial k}{\partial x_j}\right] \tag{4}$$

Received 26 October 2005; accepted for publication 6 March 2006.

*Chief CFD Developer, Advanced Simulation Technologies.

$$\frac{D\varepsilon}{Dt} = \rho\left(\frac{C_{\varepsilon 1}P_k - C_{\varepsilon 2}\varepsilon}{\tau}\right) + \frac{\partial}{\partial x_j}\left[\left(\nu + \frac{\nu_t}{\sigma_\varepsilon}\right)\frac{\partial \varepsilon}{\partial x_j}\right] \tag{5}$$

$$\frac{D\zeta}{Dt} = f - \frac{\zeta}{k}P_k + \frac{\partial}{\partial x_j}\left[\left(\nu + \frac{\nu_t}{\sigma_\zeta}\right)\frac{\partial \zeta}{\partial x_j}\right] \tag{6}$$

These equations are solved in conjunction with an equation for the elliptic relaxation function f which is formulated by using the pressure-strain model of Speziale et al. [9] (SSG) and given as

$$L^2\nabla^2 f - f = \frac{1}{\tau}\left(c_1 + C_2'\frac{P_k}{\varepsilon}\right)\left(\zeta - \frac{2}{3}\right) - \left(\frac{C_4}{3} - C_5\right)\frac{P_k}{k} \tag{7}$$

where f goes to zero at the wall:

$$f_{\text{wall}} = \lim_{y\to 0}\frac{-2\nu\zeta}{y^2}$$

and the length scale L is obtained from

$$L = C_L \max\left(\min\left(\frac{k^{3/2}}{\varepsilon}, \frac{k^{1/2}}{\sqrt{6}C_\mu S\zeta}\right), C_\eta\left(\frac{\nu^3}{\varepsilon}\right)^{1/4}\right) \tag{8}$$

Hanjalic et al. [7] neglected the last term in Eq. (7) due to small values of $(C_4/3 - C_5) \approx 0.008$. Note that Eq. (7) can be redefined by using different pressure-strain rate models, e.g., the model of Launder et al. [10], as it was done in the work of Laurence et al. [8], etc. Some other proposals can be simply integrated in Eqs. (6) and (7), e.g., so called rescaled elliptic relaxation formulation of Manceu et al. [11] where the relaxation function, Eq. (7), is rescaled with the isotropic dissipation rate as well (see original reference). Furthermore, one could make simplifications to satisfy zero wall boundary conditions for f_{wall} as proposed by Lien and Kalitzin [12].

Hanjalic et al. [7] also decreased C_2' from the original SSG value 0.9 to 0.65 to take into account the discrepancy in the definition of ε in the log-law region. The ζ–f model is very robust and more accurate than the simpler two-equation eddy viscosity models. Nevertheless, the model is usable for a relatively coarse mesh next to the wall, but again the cell next to the wall should reach a nondimensional wall distance y^+ as a maximum less than 3. The largest error is introduced when the first computational cell fails in the buffer region, e.g., $5 \le y^+ < 30$. Some authors have combined the integration up to the wall with wall functions, e.g., Esch and Menter [4], Bredberg and Davidson [13]. These smoothing functions which blend two formulations together are known as automatic wall treatment, hybrid, or compound wall treatment, etc. Popovac and Hanjalic [5] (see also Kader [14]) proposed the blending formula for the quantities specified at the cell P next to the wall as

$$\phi_P = \phi_\nu e^{-\Gamma} + \phi_t e^{-1/\Gamma} \tag{9}$$

where ν is the viscous and t the fully turbulent value of the variables wall shear stress, production, and dissipation of the turbulence kinetic energy. Popovac and Hanjalic [5] used different functions Γ for the wall shear stress and the production of turbulence kinetic energy and Γ' for the dissipation rate (see original reference), thus

$$\Gamma = \frac{0.01(P_r y^+)^4}{1 + 5P_r^3 y^+} \quad \text{and} \quad \Gamma' = \frac{0.001 y^{+4}}{1 + y^+} \tag{10}$$

where y^+ is the normalized distance to the wall.

However, Basara [15] found that a better agreement with the measurements is reached if Eq. (9) is used for the wall shear stress and the production rate, but not for the dissipation rate which is scaled as

$$\alpha = P_t/P_P \tag{11}$$

where

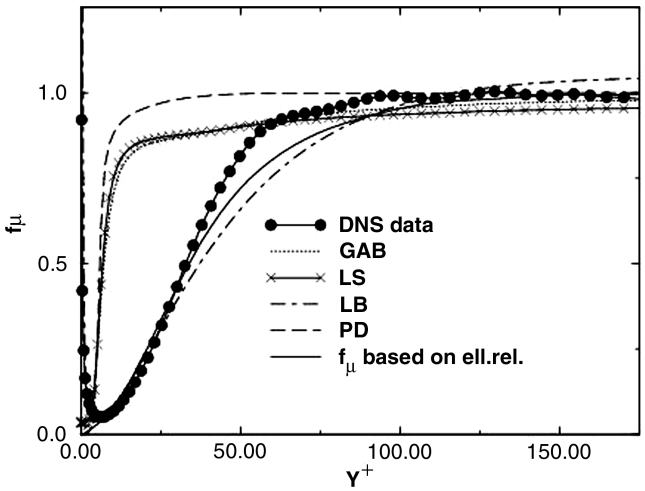

Fig. 1 Comparisons of various f_μ functions.

$$P_P = \underbrace{\tau_\nu\left(\frac{\partial U}{\partial y}\right)_P e^{-\Gamma}}_{P_\nu} + \underbrace{\tau_t\left(\frac{\partial U}{\partial y}\right)_P e^{-1/\Gamma}}_{P_t} \tag{12}$$

and P_ν, P_t are the production of turbulent kinetic energy resulting from the near wall and fully turbulent expressions for the turbulent stress, τ_ν and τ_t, respectively. This gives

$$\varepsilon_P = (1-\alpha)\frac{2\nu k_P}{y_P^2} + \alpha\frac{c_\mu^{3/4}k_P^{3/2}}{\kappa y_P} \tag{13}$$

where y_P denotes the normal distance from the near-wall cell P to the wall. The preceding equations represent the status prior to this work. The model formulated here starts from Eq. (1), thus

$$\nu_t = C_\mu\zeta\frac{k^2}{\varepsilon} = \zeta\frac{C_\mu}{c_\mu}c_\mu\frac{k^2}{\varepsilon} = \zeta\frac{C_\mu}{c_\mu}\tilde{\nu}_t = C_{\tilde{\nu}}\zeta\tilde{\nu}_t = f_\mu\tilde{\nu}_t \tag{14}$$

where

$$f_\mu = C_{\tilde{\nu}}\zeta \tag{15}$$

and $c_\mu = 0.09$, and therefore $C_{\tilde{\nu}} = 2.444$. Figure 1 shows very good agreement of such a wall damping function compared to direct numerical simulation (DNS) data for the channel flow at $Re_\tau = 395$ based on friction velocity and channel half-width (Kim et al. [16]) and with some frequently used low-Reynolds number models. The different low-Reynolds models are compared. For example, the Lam and Bremhorst [17] model (LB) employs wall distance explicitly while the Launder and Sharma [18] model (LS) employs second order normal to wall derivatives of velocity in the dissipation equation which may deteriorate the convergence rate, especially if the fine grid is not used to resolve them. Goldberg et al. [19] (GAB) offered a practical and robust model without wall normal distance but results are not in good agreement with DNS data as obtained by using Eq. (15). The equation for $\tilde{\nu}_t$ is derived from

$$\frac{D\tilde{\nu}_t}{Dt} = \frac{2c_\mu k}{\varepsilon}\frac{Dk}{Dt} - c_\mu\frac{k^2}{\varepsilon^2}\frac{D\varepsilon}{Dt} = \frac{2\tilde{\nu}_t}{k}\frac{Dk}{Dt} - \frac{\tilde{\nu}_t^2}{c_\mu k^2}\frac{D\varepsilon}{Dt} \tag{16}$$

and inserting Eqs. (4) and (5) in Eq. (16) and replacing ε in terms of k and $\tilde{\nu}_t$ (see Peng and Davidson [3]) yields

$$\begin{aligned}\frac{D\tilde{\nu}_t}{Dt} &= C_{\tilde{\nu}_{t1}}\frac{\tilde{\nu}_t}{k}P_k - C_{\tilde{\nu}_{t2}}k - C_{r1}\frac{\partial\tilde{\nu}_t}{\partial x_j}\frac{\partial\tilde{\nu}_t}{\partial x_j} + C_{r2}\frac{\tilde{\nu}_t}{k}\frac{\partial\tilde{\nu}_t}{\partial x_j}\frac{\partial k}{\partial x_j}\\ &\quad - C_{r3}\left(\frac{\tilde{\nu}_t}{k}\right)^2\frac{\partial k}{\partial x_j}\frac{\partial k}{\partial x_j} + \frac{\partial}{\partial x_j}\left[\left(\nu + \frac{\nu_t}{\sigma_{\tilde{\nu}_t}}\right)\frac{\partial\tilde{\nu}_t}{\partial x_j}\right]\end{aligned} \tag{17}$$

And Eq. (4) gets the form

$$\frac{Dk}{Dt} = P_k - C_k \frac{k^2}{\tilde{\nu}_t} + \frac{\partial}{\partial x_j}\left[\left(\nu + \frac{\nu_t}{\sigma_k}\right)\frac{\partial k}{\partial x_j}\right] \tag{18}$$

Equations (17) and (18) together with the following equations:

$$\nu_t = f_\mu \tilde{\nu}_t \tag{19}$$

$$\frac{D\zeta}{Dt} = f - \frac{\zeta}{k}P_k + \frac{\partial}{\partial x_j}\left[\left(\nu + \frac{\nu_t}{\sigma_\zeta}\right)\frac{\partial \zeta}{\partial x_j}\right] \tag{20}$$

$$L^2\nabla^2 f - f = \frac{1}{\tau}\left(c_1 + C_2'\frac{P_k}{\varepsilon}\right)\left(\zeta - \frac{2}{3}\right) \tag{21}$$

represent a new k–$\tilde{\nu}_t$–ζ–f model proposed here [note that ε in Eqs. (4) and (5) is replaced with

$$C_k \frac{k^2}{\tilde{\nu}_t}$$

where $C_k = c_\mu = 0.09$]. An advantage of this model is the simple boundary condition for the eddy viscosity, being zero on the wall and in the far field. Furthermore, a so-called compound wall treatment is simplified as Eq. (9) should be adopted for the wall boundary of the momentum equation (wall turbulent eddy viscosity or wall shear stress) as

$$U^+ = y^+ e^{-\Gamma} + \frac{1}{\kappa}\,\ell n\,(Ey^+)e^{-1/\Gamma} \tag{22}$$

$$\nu_{\text{wall}} = \nu \frac{y_P^+}{U_P^+} \tag{23}$$

and now only for the production of turbulence kinetic energy as given in Eq. (12).

The proposed model is very simple and although new, it has already been well tested. It differs from the Peng and Davidson model [3] in the damping function f_μ which is again used from the well-tested modeling approach advanced by Durbin [6] and many authors afterwards, e.g., Hanjalic et al. [7]. It should also be clear that f_μ is not limited with the maximum value equal 1; it varies in the flowfield according to the variation of ζ. However, the main difference will appear in the near-wall region due to the adopted compound wall treatment and the damping function f_μ. Constants in $\tilde{\nu}_t$ and k are used as derived by Peng and Davidson [3]: $C_{\tilde{\nu}_{t1}} = 0.4$, $C_{\tilde{\nu}_{t2}} = 0.018$, $C_k = 0.09$, $C_{r1} = 1.2$, $C_{r2} = 1.17$, $C_{r3} = 0$, $\sigma_{\nu t} = 1.2$, and $\sigma_k = 1.2$. The other constants in Eqs. (20) and (21) are used as given in Hanjalic et al. [7]: $c_1 = 0.40$, $C_2' = 0.65$, and $\sigma_\zeta = 1.2$. The model is completed by imposing the Kolmogorov time and length scale as the lower bounds as

$$\tau = \max\left(\frac{\tilde{\nu}_t}{c_\mu k}, C_\tau\left(\frac{\nu\tilde{\nu}_t}{k^2}\right)^{1/2}\right) \tag{24}$$

$$L = \max\left(\frac{\tilde{\nu}_t}{c_\mu k^{1/2}}, C_\eta\left(\frac{\nu^3\tilde{\nu}_t}{k^2}\right)^{1/4}\right) \tag{25}$$

where the constants are $C_\tau = 20$ and $C_\eta = 155.19$. Note that original values proposed by Hanjalic et al. [7], $C_\tau = 6$, $C_\eta = 85$, are scaled with $1/c_\mu^{1/2}$ and $1/c_\mu^{1/4}$, respectively, due to

$$\varepsilon = c_\mu \frac{k^2}{\tilde{\nu}_t}$$

III. Results and Discussions

The performance of the methodology described above is assessed here in the following examples: a plane channel and a 180° turnaround duct. Direct numerical simulation data of Kim et al. [16] for the fully developed turbulent flow in a plane channel at $Re_\tau = 395$ were used for comparisons. Three different computational grids

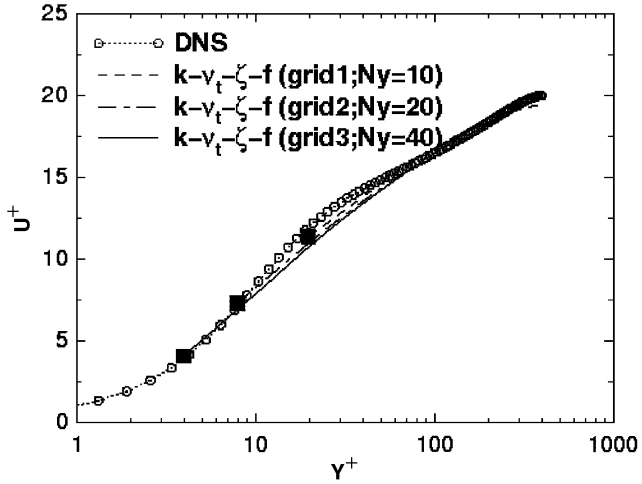

Fig. 2 Computed mean velocity in a plane channel by using three different computational grids. Symbols: DNS, Kim et al. [16].

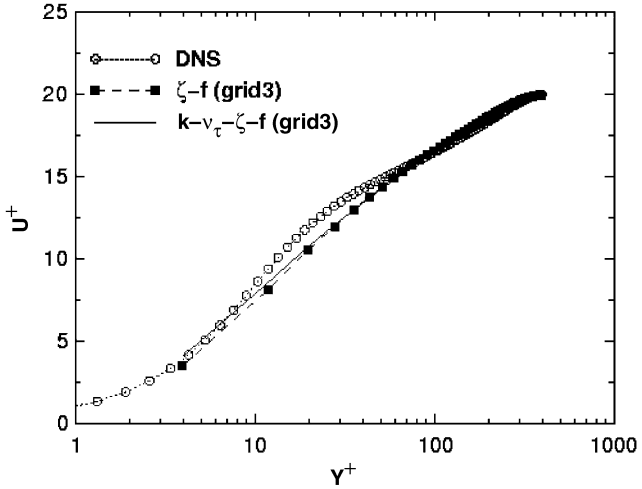

Fig. 3 Computed mean velocity in a plane channel with the ζ–f and k–$\tilde{\nu}_t$–ζ–f in conjunction with compound wall treatment. Symbols: DNS, Kim et al. [16].

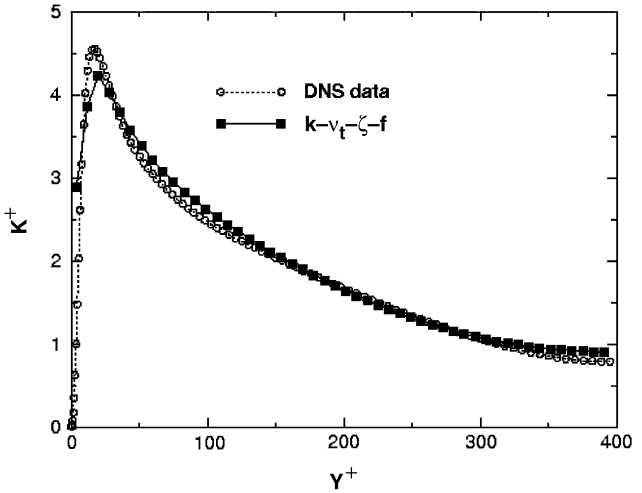

Fig. 4 Computed turbulence kinetic energy in a plane channel with the k–$\tilde{\nu}_t$–ζ–f model. Symbols: DNS, Kim et al. [16].

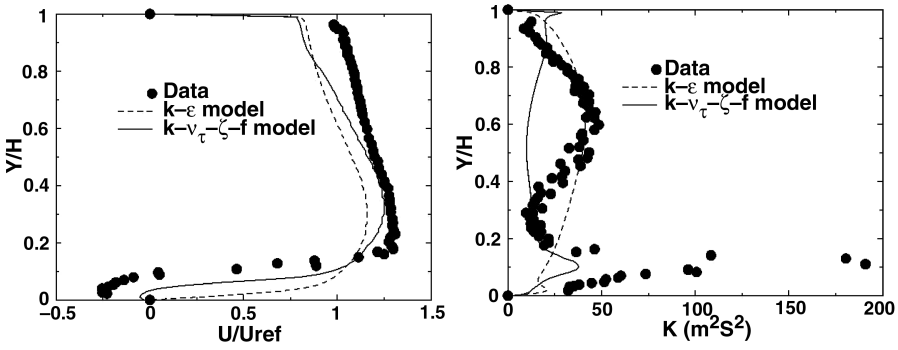

Fig. 5 Profiles at a selected location along the flow in a 180° turned U-bend at 180°: a) mean velocity, b) turbulence kinetic energy.

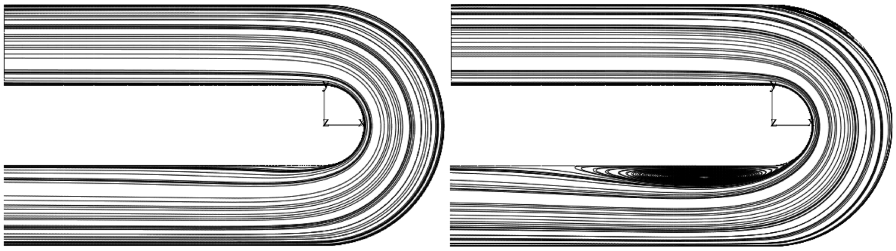

Fig. 6 Streamline patterns of the flow in a of 180° turned U-bend obtained by a) the k–ε model and b) the k–$\tilde{\nu}_t$–ζ–f model.

were employed, each having twice as much in the normal to wall direction: 10, 20, and 40 cells for half of the channel (uniformly distributed cells). The log law considering velocity distribution for each of the grids is well captured as shown in Fig. 2. Note that the aim of this test case is to predict the log law by having relatively high y^+ values, e.g., above 3 (see the black filled boxes which marks the start of each curve in Fig. 2), so that the compound wall treatment is used for the interpolation in the buffer layer.

The difference between ζ–f and k–$\tilde{\nu}_t$–ζ–f predictions is negligible for the finest grid as shown in Fig. 3. The distribution of turbulence kinetic energy is also well captured; see Fig. 4. This shows that the model proposed here in conjunction with the simplified compound wall treatment is fairly independent of the grid distribution next to the wall.

The second example is based on the data of Monson et al. [20] in a 180° turnaround duct formed from a rectangular channel with an aspect ratio of 10. The flow is two dimensional along the midplane and the results obtained in this work are reported for the Reynolds number of 10^6. The results predicted with the k–ε model are identical to the predictions of Basara [21] who reported a grid independent solution and are very similar to other model's performances reported elsewhere, e.g., Shur et al. [22]. Therefore, the grid of 22,000 computational cells used in this work is sufficiently fine not to influence turbulence models testing (additionally two numerical grids were used with 8736 and 17,472 cells as reported by Basara et al. [23]). The second order convection scheme MINMOD was used for all calculations presented here (Przulj and Basara [24]). The challenge for the turbulence models is to predict the separation region after the bend. Figures 5a and 5b compare the predicted and measured axial mean-velocity and turbulence kinetic energy profiles at 180°.

The k–$\tilde{\nu}_t$–ζ–f model captures the velocity profile shape better than the k–ε model and the flow clearly separates as shown in Fig. 6 where the predicted streamlines are compared. The level of turbulence kinetic energy is underpredicted but similar results are obtained even by using the full Reynolds-stress model as shown in the work of Basara [21]. However, closer agreement is achieved with the k–$\tilde{\nu}_t$–ζ–f model. Note that the k–ε model was also used in conjunction with the compound wall treatment.

IV. Conclusions

The new k–$\tilde{\nu}_t$–ζ–f model is proposed based on the solution of the k and $\tilde{\nu}_t \sim k^2/\varepsilon$ equations and wall damping function f_μ obtained by solving the $\zeta = \overline{v^2}/k$ equation. Zero values as wall boundary conditions can be used for all equations: k, $\tilde{\nu}_t$, and ζ. The model is implemented in conjunction with the simple wall blending approach combining the integration up to the wall with the wall function. Replacing the ε equation with the $\tilde{\nu}_t$ equation removes all arbitrariness about implementing the compound wall treatment. This approach shows less sensitivity on the distribution of the computational cells next to the wall. Future work will check if the model can be further simplified by removing some of the diffusion like terms in the $\tilde{\nu}_t$ equation (those with constants C_{r1}, C_{r2}) and modifying the remaining constants to compensate for the omission of these terms.

References

[1] Speziale, C. G., Abid, R., and Anderson, E. C., "Critical Evolution of Two-Equation Models for Near Wall Turbulence," *AIAA Journal*, Vol. 23, No. 2, 1992, pp. 324–331.

[2] Wilcox, D., "Reassessment of the Scale-Determining Equation for Advanced Turbulence," *AIAA Journal*, Vol. 26, No. 11, 1988, pp. 1299–1310.

[3] Peng, S. H., and Davidson, L., "New Two-Equation Eddy Viscosity Transport Model for Turbulent Flow Computation," *AIAA Journal*, Vol. 38, No. 7, 2000, pp. 1196–1205.

[4] Esch, T., and Menter, R. F., "Heat Transfer Predictions Based on Two-Equation Turbulence Models With Advanced Wall Treatment," *Proceedings of the 4th International Symposium on Turbulence, Heat and Mass Transfer*, edited by K. Hanjalic, Y. Nagano, and M. Tummers, Vol. 4, Begell House, 2003, pp. 633–640.

[5] Popovac, M., and Hanjalic, K., "Compound Wall Treatment for RANS Computation of Complex Turbulent Flows," *Proceedings of the Third MIT Conference On Computational Fluid and Solid Mechanics*, edited by K. Bathe, Vol. 1, Elsevier, New York, 2005, pp. 802–806.

[6] Durbin, P. A., "Near-Wall Turbulence Closure Modelling Without Damping Functions," *Theoretical Computational Fluid Dynamic*, Vol. 3, 1991, pp. 1–13.

[7] Hanjalic, K., Popovac, M., and Hadziabdic, H., "A Robust Near-Wall Elliptic-Relaxation Eddy-Viscosity Turbulence Model for CFD,"

International Journal of Heat and Fluid Flow, Vol. 25, No. 6, 2004, pp. 1048–1051.

[8] Laurence, D. R., Uribe, J. C., and Utyuzhnikov, S. V., "A Robust Formulation of the v2-f Model," *Flow, Turbulence and Combustion*, Springer, The Netherlands, Vol. 73, No. 3, 2004, pp. 169–185.

[9] Speziale, C. G., Sarkar, S., and Gatski, T. B., "Modeling the Pressure-Strain Correlation of Turbulence, an Invariant Dynamical Systems Approach," *Journal of Fluid Mechanics*, Vol. 227, 1991, pp. 245–272.

[10] Launder, B. E., Reece, G., and Rodi, W., "Progress in the Development of a Reynolds Stress Turbulence Closure," *Journal of Fluid Mechanics*, Vol. 68, 1975, pp. 537–566.

[11] Manceau, R., Carlson, J. R., and Gatski, T. B., "A Rescaled Elliptic Relaxation Approach: Neutralizing the Effect on the Log Layer," *Physics of Fluids*, Vol. 14, No. 11, 2002, pp. 3868–3879.

[12] Lien, F. S., and Kalitzin, G., "Computation of Transonic Flows With the $\overline{v^2} - f$ Turbulence Model," *International Journal of Heat and Fluid Flow*, Vol. 22, No. 1, 2001, pp. 53–61.

[13] Bredberg, J., and Davidson, L., "Low-Reynolds Number Turbulence Models: An Approach for Reducing Mesh Sensitivity," *Journal of Fluids Engineering*, Vol. 126, No. 1, 2004, pp. 14–21.

[14] Kader, B. A., "Temperature and Concentration Profiles in Fully Turbulent Boundary Layers," *International Journal of Heat and Mass Transfer*, Vol. 24, 1981, pp. 1541–1544.

[15] Basara, B., "Calculation of Vortex Shedding From a Circular Cylinder in a Uniform and Shear Flows," ASME Paper FED2005-77431, 2005.

[16] Kim, J., Moin, P., and Moser, R., "Turbulence Statistics in Fully Developed Channel Flow at the Low Reynolds Number," *Journal of Fluid Mechanics*, Vol. 177, 1987, pp. 133–166.

[17] Lam, C. K. G., and Bremhorst, K., "A Modified Form of the $k - \varepsilon$ Model for Predicting Wall Turbulence," *Journal of Fluids Engineering*, Vol. 103, 1981, pp. 456–460.

[18] Launder, B. E., and Sharma, B. I., "Application of the Energy-Dissipation Model of Turbulence to the Calculation of Flow near a Spinning Disk," *Letters in Heat and Mass Transfer*, Vol. 1, 1974, pp. 131–138.

[19] Goldberg, U., Apsley, D., and Batten, P., "A Wall-Distance Free Low-Reynolds $k - \varepsilon$ Model," *Proceedings of the Flow Modeling and Turbulence Measurements VI*, edited by C. J. Chen, C. Shih, J. Lienau, and R. J. Kung, Balkema Publishers, 1996, pp. 249–256.

[20] Monson, D. J., Seegmiller, H. L., and McConnaughey, P. K., "Comparison of LDV measurements and Navier-Stokes Equations in a Two-Dimensional 180-Degree Turn-Around Duct," AIAA Paper 89-0275, 1989.

[21] Basara, B., "Employment of the Second-Moment Turbulence Closure on Arbitrary Unstructured Grids," *International Journal for Numerical Methods in Fluids*, Vol. 44, No. 4, 2004, pp. 377–407.

[22] Shur, M. L., Strelets, M. K., Travin, A. K., and Spalart, P. R., "Turbulence Modelling in Rotating and Curved Channels: Assessing the Spalart-Shur Correction," *AIAA Journal*, Vol. 38, No. 5, 2000, pp. 784–792.

[23] Basara, B., Cokljat, D., and Younis, B. A., "Assessment of Eddy-Viscosity and Reynolds-Stress Transport Closures in Two- and Three-Dimensional Turn-Around Ducts," *Proceedings of the Symposium on Separated and Complex Flows*, ASME FED, edited by M. V. Otugen, Vol. 217, 1995, pp. 249–256.

[24] Przulj, V., and Basara, B., "Bounded Convection Schemes for Unstructured Grids," AIAA Paper 2001-2593, 2001.

P. Givi
Associate Editor